ISSN: 2350-0328

International Journal of AdvancedResearch in Science, Engineering and Technology

Vol. 5, Issue 6 , June 2018

Structural investigation, DFT, biological studies of binuclear Hg(II) complex of big dithiosemicarbazide derived from 2-benzylmalonohydrazide

R. M. El-Morshedy, M. M. Abou-Elzahab , G. M. Abu El-Reash*

Department of Chemistry, Faculty of Science, Mansoura University, Mansoura, Egypt.

ABSTRACT: The binuclear Hg(II) complex of *N*,*N'*-(2,2'-(2-benzylmalonyl)bis(hydrazine-1-carbonothioyl))dibenzamide (H_4BPCD), which derived from the combination of 2-benzylmalonohydrazide suspension with benzoyl-isothiocyanate, have been isolated and investigated by the necessary analytical and spectroscopic techniques. The IR studies show that H_4BPCD disposebi-negative tetradentate O S donor *via* two thione S of (C=S) group and two deprotonated enolic (C-O) groups in the prepared complex. Biological studies of minimum inhibitory concentration and *in vitro* determination of SOD-like activity were tested for the ligand and its complex.

KEYWORDS: Thiosemicarbazide; spectral characterization; DFT molecular modeling; MIC and SOD-like activity.

I.INTRODUCTION

The N-, O- and S- containing ligands of dihydrazide derivatives that can chelate with two metal ions have become important because of symmetric and asymmetric binuclear complexes exhibited a variety of stereochemistries and bonding behaviors and that produce diverse structures and properties [1-3]. Several studies have been carried out on the binuclear complexes because the flexible separation part of the metal ion in the molecule have several interesting applications like creation of supramolecular structures to mimic metalloproteins [4], DNA binding, specific and selective catalysis [5, 6], sequestering of metal ions and other of both biological and industrial applications. In *vitro* and in *vivo* tests [7] proved dihydrazides to be non-genotoxic, anti-inflammatory, antioxidant and anticancer activities [8-10]. Also, their derivatives in the field of analytical chemistry used as reagents for specific chemical separations [11-13], spectrophotometric micro determination of some metal ions [14-16] and used for polymer industry [17, 18]. Furthermore, luminescent compounds are very interesting because of their many applications for photocatalysis [19-22]. In order to share to these studies we have prepared *N*,*N'*-(2,2'-(2-benzylmalonyl)bis(hydrazine-1-carbonothioyl))dibenzamide (H_4BPCD) and its Hg(II) complex. We apply geometry optimization (using Materials Studio package [23]) and conformational analysis to the H_4BPCD and all their possible structural isomers and have got the more stabilized. The proposed structures were upheld by DFT molecular modeling. Other studies carried out such as spectroscopic (IR, UV-vis,^{1}H and ^{13}C NMR) and biological (MIC efficacies and SOD-like activity).

II. EXPERIMENTAL

A. Materials and Instrumentation.

The diethyl 2-benzylmalonate and hydrazine were purchased from Cambrian and Fluka and used as received. The analysis of C, H and N is carried out with a "Perkin–Elmer 2400 series II analyzer". The metal and chloride contents in prepared complex were determined by traditional methods [24]. "Fisher-Johns melting point apparatus" is used for melting points (^{o}C) determination and are uncorrected. The ^{1}H and ^{13}C NMR spectrum of H_4BPCD at room temperature was recorded on a Varian Gemini spectrometer (400 MHz) in d^6-DMSO at Faculty of Science, KafrElsheikh University using tetramethylsilane as an internal standard. IR spectra (4000–400 cm^{-1}) with KBr discs were recorded on a Mattson 5000 FTIR spectrophotometer, at Mansoura University. The electronic spectra of the complexes have been measured in the range 200-900 nm in DMSO solution on a Perkin Elmer Lamda 25 UV/Vis Spectrophotometer, at Mansoura University.

ISSN: 2350-0328

International Journal of AdvancedResearch in Science, Engineering and Technology

Vol. 5, Issue 6 , June 2018

B. Synthesis of H_4BPCD

The ligand was prepared in two main steps: Step1, by mixing 1: 2 molar ratio of diethyl 2-benzylmalonate (2.35 g, 0.01mol) and hydrazine (0.486 g, 0.02 mol) with stirring for 2 minutes then adding 30 ml ethanol to the mixture followed by reflux for 2-3 h, then the contents were poured in a beaker and left overnight. The solvent is removed by filtration and the residue washed by diethylether. Step2, suspension of the result compound (2-benzylmalonohydrazid) (2.0891 g) in ethanol (15 ml) was added to ethanolic solution of 2.7 ml benzoyl isothiocyanate and refluxed for 3-4 h, then the precipitate (H_4BPCD) washed by diethyl ether after filtration.
At the end of each step, the result compound was desiccated over anhydrous $CaCl_2$ and checked by TLC. The melting points of the hydrazide and H_4BPCD (structure 1) found to be 167 and 220 ºC, respectively.

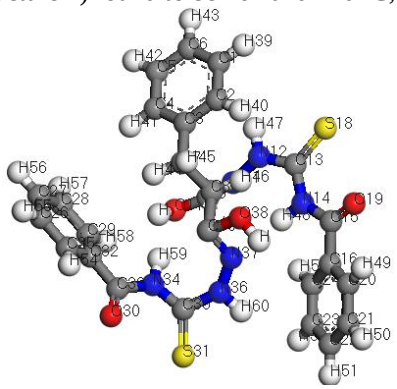

Structure1: Molecular modeling of H_4BPCD_{enol}

C. Synthesis of Hg(II) complex.

The chloride salt of mercury (1.02 mmol) dissolved in hot ethanol (30 ml) and then added to a hot ethanolic suspension of H_4BPCD (1.02 mmol). The contents were refluxed for 4 h. The fine formed precipitate was filtered and washed with ether and then desiccated over $CaCl_2$. The complex powder give yield of 90%, and the proposed structures are supported by analytical and spectroscopic data (Table 1).

Table 1. Analytical and physical data of H_4BPCD and its metal complex.

Compound	M.wt.	Colour	M.p.; °C	% Found (Calcd.)					Yield%
				M	Cl	C	H	N	
(H_4BPCD) $C_{26}H_{24}N_6O_4S_2$	548.64	White	220	—	—	62.05 (62.99)	4.45 (4.22)	15.54 (15.32)	95
$[Hg_2(H_2BPCD)Cl_2(H_2O)_2]$ $C_{26}H_{26}Hg_2N_6O_6S_2$	1054.73	Paige	280	38.12 (38.04)	6.52 (6.72)	29.58 (29.61)	2.91 (2.48)	7.95 (7.97)	90

D.Computational details

So as to get insight to the structural stabilities of the prepared compounds, DFT calculations with periodic boundary conditions were performed with the DMol^3[25] code, using Materials Studio package [23]. All the functions were used in conjunction with the precise double numerical plus polarization basis set DNP which is overweight the accuracy of that Gaussian basis set [26]. The RPBE functional [27] is so far the best exchange-correlation functional [28], in the light of the generalized gradient approximation (GGA), is utilized to assess the exchange and relationship effects of electrons. The geometric optimization is done with no symmetry limitation.

E. Biology

1. Minimum inhibitory concentration (MIC)

The potencies of H_4BPCD and its complex as antibacterial and antifungal were examined by diffusion method of agar and potato dextrose, respectively [29]. The examination was carried out in DMSO at 100, 200 and 500 µg/ml by using two bacteria (*Escherichia coli* as Gram-negative bacteria and *Staphylococcus aureus* as Gram-positive bacteria) and one fungi (*Candida albicans*) by the MIC method [30]. These bacterial strains were incubated for 24h at 37ºC while

ISSN: 2350-0328

International Journal of AdvancedResearch in Science, Engineering and Technology

Vol. 5, Issue 6 , June 2018

fungi strain was hatched for 48h. at 37ºC. The Ampicillin and Clotrimazole as standards were utilized for examination at the same conditions. Efficacy was estimated by diameter measuring of complete inhibition zone (mm).

2. Antioxidant activity (Determination of SOD-like activity)

Free ligand (H_4BPCD) and its complex were investigated for superoxide dismutase (SOD)-like activity using well-known method [31]. The solutions of H_4BPCD and/or its isolated complex were prepared in DMSO. The response was started by phenazine methosulfate (PMS) addition, and the expansion in absorbance at 560 nm was recorded by the spectrophotometer for 5 minutes. For relative purposes, the activity of native L-Ascorbic acid has also been resolved .

III. RESULTS AND DISCUSSION

A. IR Spectra of H_4BPCD and its metal complex

The IR spectral data provide us by the valuable information regarding functional groups. The main characteristic frequencies of H_4BPCD (Figure 1a) and its Hg(II) complex (Figure 1b) are summarized in Table 2. Because the symmetrical nature of both sides in the ligand and complexes, one absorption band is observed for most of the functional groups except when the environment varies because of chelation.

Table 2: Assignment of the IR spectral bands of H_4BPCD and its metal complex.

Compound	υ(OH)	$\upsilon(C=N)_1$	$\upsilon(C=O)_2$	$\upsilon(C\text{-}O)_1$	δ(C=S)	$\upsilon(C=N)_2^*$	υ(C=C)	υ(N-N)	$\upsilon(NH)_a$	$\upsilon(NH)_b$
H_4BPCD	3223	1602	1687	1252	850	-	1527	980	3191	3061
$[Hg_2(H_2BPCD)Cl_2(H_2O)_2]$	-	-	-	-	891	1564	1494	1002	3196	3060

The ligand exhibits broad band of medium intensity at 3223 cm^{-1} assigned for υ(OH) and sharp intense band at 1687 cm^{-1} may be due to overlapping of $\upsilon(C=O)_1$ and $\upsilon(C=O)_2$ bands. Appearance of υ(C-O) band at 1252 cm^{-1} in addition of two mentioned bands pointed to the presence of H_4BPCD in the two forms (keto and enol) which confirmed also by ^1H and ^{13}C NMR spectral analysis. The vibrations of $(NH)_a$ and $(NH)_b$ lies at 3191 and 3061 cm^{-1} and the band at 1602 cm^{-1} referred to $\upsilon(C=N)_1$ [32, 33].

The $\upsilon(C=O)$, $\upsilon(C=N)_1$ and υ(OH) bands have been disappeared in the IR spectrum of Hg(II) complex (Structure 2). The δ(C=S) band undergoing blue shifted in the prepared complex due to the sharing in coordination. Because of enolization of $(C=O)_2$ group and coordination from deprotonated (OH) group, new $\upsilon(C=N)_2^*$ vibrational band has been appeared clearly in the Hg(II) complex at 1564 cm^{-1}. Stretching vibration band of (N-N) bond shifted to upward in the metal complex due to involvement of neighboring (C=S) group [34]. The medium band of $\upsilon(NH)_a$ vibration remains unaltered in Hg(II) complex confirming the suggested structure for the complex. In addition, $\upsilon(NH)_b$ appears around the region of 3060 cm^{-1} confirming un-participation in the chelation. The new low frequency non-ligand bands at 531, 456 cm^{-1} were assigned to υ(M-Cl) [35] and υ(M-O), respectively.

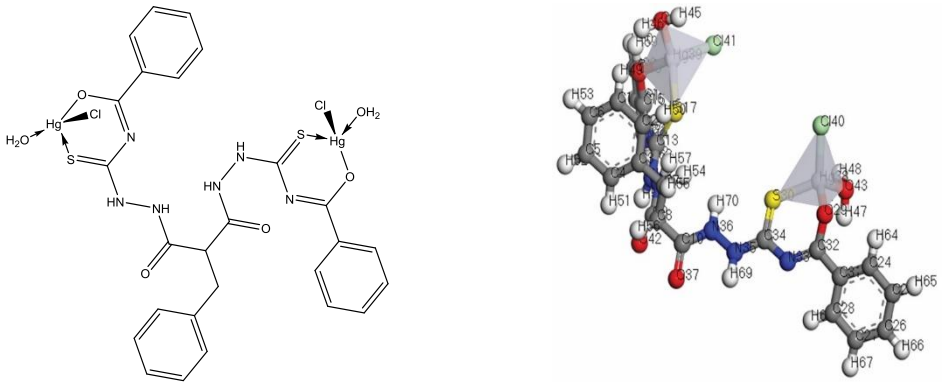

Structure 2: The 2D structure/3D molecular modeling of $[Hg_2(H_2BPCD)Cl_2(H_2O)_2]$ complex.

ISSN: 2350-0328

International Journal of AdvancedResearch in Science, Engineering and Technology

Vol. 5, Issue 6 , June 2018

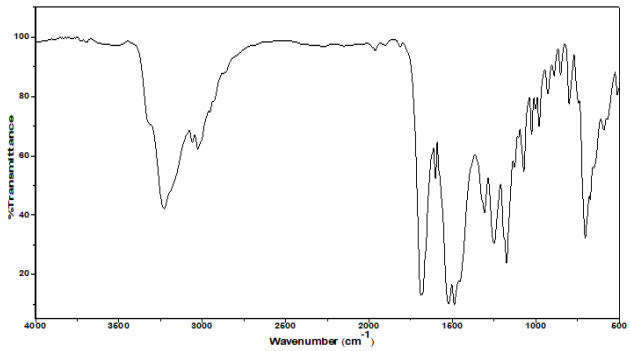

(a) Infrared spectrum H_4BPCD ligand.

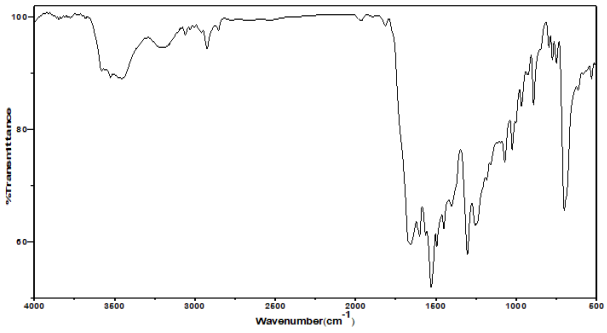

(b) Infrared spectrum of $[Hg_2(H_2BPCD)Cl_2(H_2O)_2]$ complex.

Figure 1

B . ^{1}H and ^{13}C NMR Spectra of the H_4BPCD.

The ^{1}H NMR spectrum of H_4BPCD (Figure 2a) shows three singlet signals at δ= 10.17, 11.19 and 11.81 ppm relative to TMS that disappear upon deuteration. These signals attributed to $(NH)_a$, $(NH)_b$ and (OH) protons respectively [36, 37]. The signals of NH groups appeared in high downfield frequencies because of formation of two hydrogen bond between N(36)-H(81) and N(11)-H(48). Appearance of (OH) signal at high frequency is additional evidence that the ligand present in enol form. The multiplets at 7.15-7.95 ppm belong to the protons of phenyl ring [38]. Doublet and triplet signals at 3.15- 3.20 and 3.92-3.98 ppm refereed to ($-CH_2$) and (-CH) groups respectively.

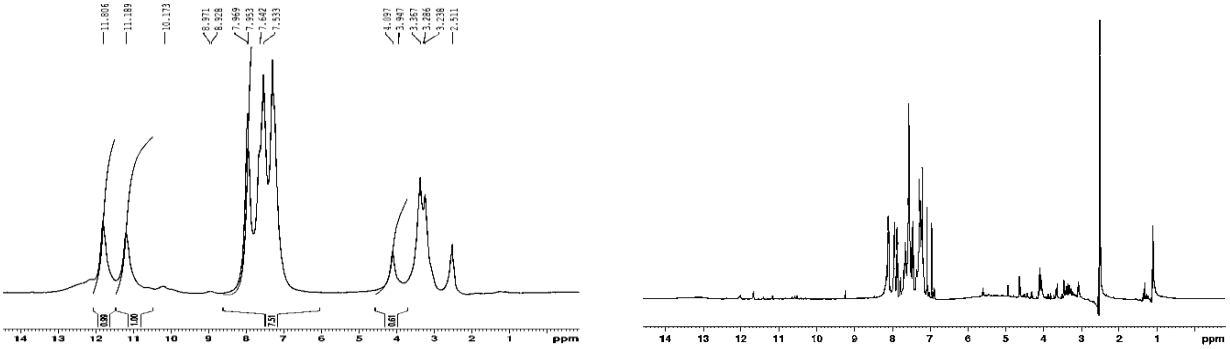

(a) ^{1}H NMR spectrum of H_4BPCD. (b) ^{1}H NMR spectrum of Hg(II) complex.

Figure 2

In the ^{1}HNMR spectrum of Hg(II) complex (Figure 2b), the (OH) signal was disappeared which confirm that ligand coordinated to metal in the enol form with deprotonation. Moreover, the signal of $(NH)_a$ appears at 11.63 ppm [39] and the signal of $(NH)_b$ appears at 12.01 ppm. Finally, phenyl protons assigned in the range of 6.93-7.53 ppm, doublet signals of ($-CH_2$) group observed around the range of 3.63-3.67 ppm and triplet signals of (-CH) group appears in the range of 3.06-3.07 ppm.

The ^{13}C NMR spectrum of H_4BPCD (Figure 3) shows two signals belong to $(C=O)_1$ and $(C=O)_2$ groups appear at δ= 172.01 and 164.55 ppm, and also a signal at δ= 175.45 ppm assigned to (C=S) group. The aromatic carbons were observed at δ= 126.92-138.66 [40]. Moreover, appearance of carbon resonance signal of (N=C-OH) at 168.68 in addition of $(C=O)_1$ signal suggest the presence of keto-enol tautomer of in solution.

ISSN: 2350-0328

International Journal of AdvancedResearch in Science, Engineering and Technology

Vol. 5, Issue 6 , June 2018

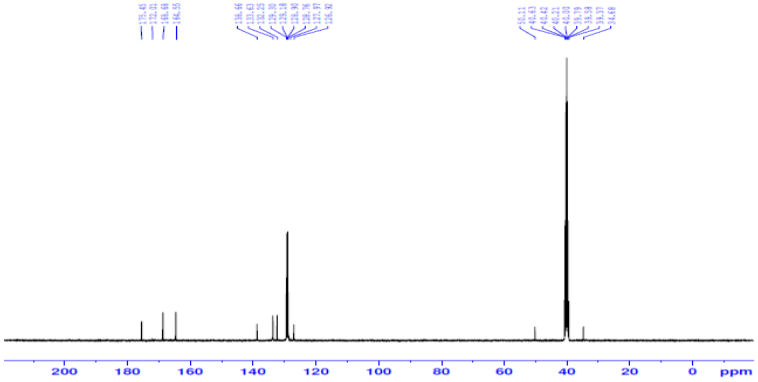

Figure 3: ^{13}C NMR spectrum of H_4BPCD.

C. Electronic Spectral Studies

The ligand H_4BPCD shows two intense bands around 307 nm (32573 cm^{-1}) and 342 nm (29240 cm^{-1}) in DMSO solution, because of the intramolecular transitions (π–π^*) and (n–π^*) respectively.

D. Molecular Modelling with DFT method:

1- IR

Frequency calculation analyses have been performed for H_4BPCD possible forms in order to ensure the most prevalent form/forms. The little difference between that experimental wavenumbers and the calculated one is may due to that the experimental wavenumbers were carried out for solid samples, while the calculations were processed in a vacuum for a free molecule as shown Table 3. It was found that the values of wavenumbers of calculated frequencies are with good agreement with experimental one, especially combination with the two graphs of form 1 (enol form) and form 3 (keto form) which confirm the presence of the two forms in the solid form of the title compound.

Table 3: Theoretical IR comparison of H_4BPCD possible forms.

Compound	υ(O-H)	$\upsilon(C=N)_1$	υ(C-O)	δ(C=S)	υ(C-S)	υ(S-H)	$\upsilon(C=O)_1$	$\upsilon(C=O)_2$	$\upsilon(C-O)_2$	$\upsilon(C=N)_2$*	υ(C=C)	υ(N-N)	$\upsilon(NH)_a$	$\upsilon(NH)_b$
H_4BPCD (experimental)	3223	1602	1252	850	-	-	-	1687	-	-	1527	980	3196	3061
H_4BPCD_{enol} form1 (theoretical)	3195	1605	1266	851	-	-	-	1657	-	-	1527	981	3195	3061
H_4BPCD form2 (theoretical)	3300	1618	1252	843	-	-	-	-	1335	1585	1521	977	3177	3062
H_4BPCD_{keto} form3 (theoretical)	-	-	-	849	-	-	1740	1680	-	-	1524	981	3182	3065
H_4BPCD form4 (theoretical)	3259	1629	1268	855	1110	1229	-	1630	1366	-	1516	986	3167	3098
H_4BPCD form5 (theoretical)	-	-	-	-	1116	1259	1783	1668	-	-	1515	958	3193	3086

The corresponding graphic (Figure 4) described harmony between the experimental and theoretical wavenumbers since the relations between them are linear and can be expressed by the next equations:

For the enol form1 $\upsilon_{cal} = 0.99425\ \upsilon_{exp} + 11.352$ with correlation coefficients $\times (R^2 = 0.99977)$.

For the keto form3 $\upsilon_{cal} = 1.01121\ \upsilon_{exp} + 23.899$ with correlation coefficients $\times (R^2 = 0.99918)$.

ISSN: 2350-0328
International Journal of AdvancedResearch in Science, Engineering and Technology
Vol. 5, Issue 6 , June 2018

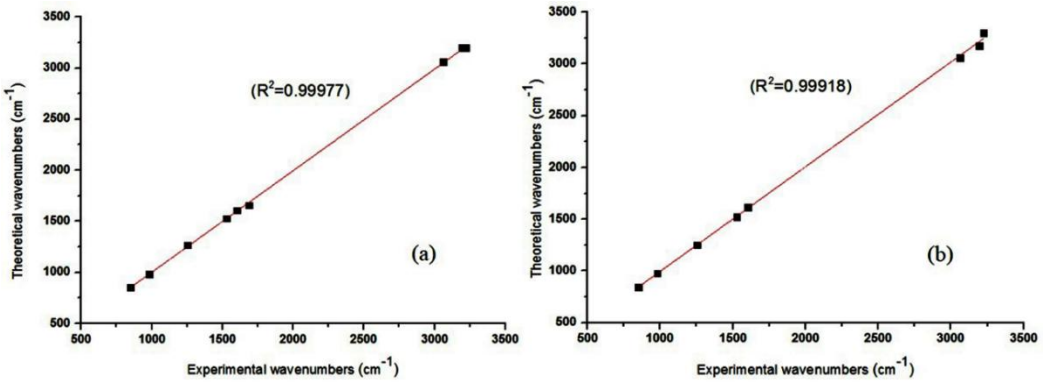

Figure 4: The linear regression between the experimental and theoretical frequencies of H_4BPCD a) for keto form3 and b) for enol form1.

2- Geometry optimization with DFT method for ligand and its possible forms

The DFT/DMoL^3 method has been used for a complete study of the molecular structures of all the possible conformations of H_4BPCD (Structures 3) in order to obtain their stability order according to the calculated energy components (Table 4). It was found that H_4BPCD form1 has the lowest total energy and highest binding energy which mean that form1 is the most stable conformation.

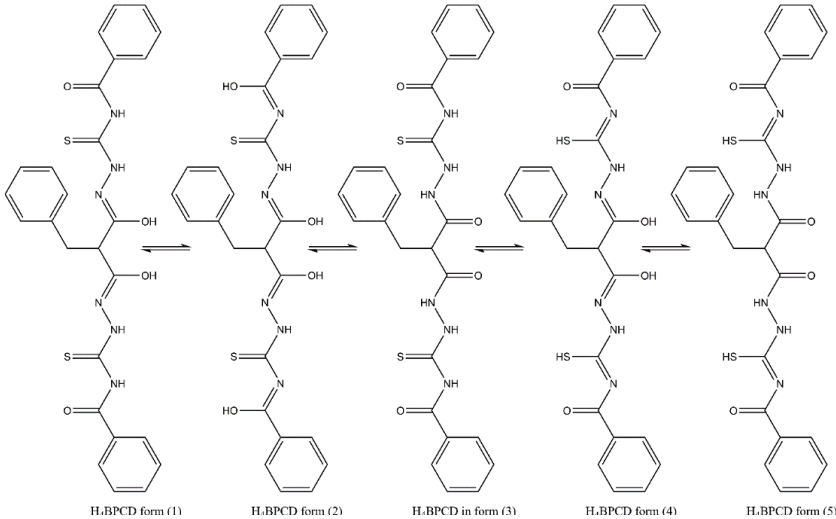

Structure 3: structure of possible conformations of H_4BPCD

Table 4: Energy component (kcal/mol) of possible forms of H_4BPCD and its Hg(II) complex.

ISSN: 2350-0328

International Journal of AdvancedResearch in Science, Engineering and Technology

Vol. 5, Issue 6 , June 2018

Compound	Energy components (kcal/mol)						Binding Energy (kcal/mol)
	Sum of atomic energies	Kinetic Energy	Electrostatic energy	Exchange-correlation energy	Spin polarization energy	Total Energy	
H_4BPCD form (1)	-1518200.4	-11886.8	-17.3	2807.0	2233.2	-15258777	-6863.9
H_4BPCD form (2)	-1518833.5	-11662.2	-548.4	2877.1	2287.9	-1525064.3	-7044.2
H_4BPCD form (3)	-1517567.4	-12209.4	582.1	2744.8	2178.4	-1524262.6	-6695.2
H_4BPCD form (4)	-1517567.4	-11863.3	260.2	2730.9	2178.4	-1524246.9	-6679.6
Hg(II) complex	-107462.1	-515.1	-49.6	136.12	35.8	-89124.8	-325.8

E. Biological studies: 1. Determination of minimum inhibitory concentration (MIC)

The H_4BPCD was initially evaluated for *in vitro* antibacterial activity against G+ve and G-vebacteria and fungal using Broth method [41]. Standard antibiotic namely Ampicillin and standard antifungal drug Clotrimazole were applied as reference drugs. It was found that H_4BPCDshow high activity against all organisms (Table 5).

Table 5: Minimal inhibitory concentration (MIC, µg/mL) of the newly synthesized compounds.

Compound	*E. coli*	*S. aureus*	*C. Albicans*
Ampicillin	125	93.7	----
Clotrimazole	----	----	5.8
H_4BPCD	187.5	125	23.4

1. Antioxidant activity (Determination of SOD-like activity)

Within a cell, the superoxide dismutases (SODs) constitute the first line of defense against ROS [42]. Therefore, SOD mimics have these great attention potential pharmaceutical agents for treating such diseases. A significant SOD-like activity was observed for H_4BPCD as represented in table 6, with inhibition percent 77.3%.

Table 6: Superoxide (SOD)-like activity of H_4BPCD and its metal complex as antioxidative enzyme.

Compound	Δ through 5 min	% inhibition
Control	0.468	0%
L-Ascorbic acid	0.101	78.4%
H_4BPCD	0.106	77.3%

% inhibition = (ΔControl- ΔTest/ΔControl)×100

IV. CONCLUSION AND FUTURE WORK

In this study the vibrational analysis, ^{1}H NMR and C^{13}NMR spectra of a newly synthesized *N*,*N*'-(2,2'-(2-benzylmalonyl)bis(hydrazine-1-carbonothioyl))dibenzamide (H_4BPCD) compound and its binuclear Hg(II)complex have been studied and characterized. The spectral analysis confirmed the presence of both forms (keto and enol) of

ISSN: 2350-0328

International Journal of AdvancedResearch in Science, Engineering and Technology

Vol. 5, Issue 6 , June 2018

H_4BPCD. A tetrahedral geometry was proposed for the Hg(II) complex. The optimized geometries have been calculated by using DFT/DMol^3 method with DNP basis set. The comparison of theoretical vibrations of H_4BPCDwith experimental data showed a good agreement. The parent compound exhibited high antimicrobial activity and SOD-like activity. Since of the H_4BPCD compound is good candidate for future pharmacological studies the obtained results will be useful in their use in these areas.

REFERENCES

[1] U.R. Bhagavatula, S. Pulipaka, S. Atreyapurapu, Int. Res. J. Pure. Appl. Chem. **2016**, *11*, 1.
[2] A. Satyanarayana, D.N. Kenie, P. Shyamala, Acta Chim. Slov. **2014**, *60*, 807.
[3] L. Tsitsishvili, T. Tsutsunava, K.Y. Ya., KoordinatsionnayaKhimiya. **1982**, *8*, 674.
[4] T.A. Kaden, Coord. Chem. Rev. **1999**, *190*, 371.
[5] H. Steinhagen, G. Helmchen, Angew. Chem. Int. Ed. **1996**, *35*, 2339.
[6] E.K. van den Beuken, B.L. Feringa, Tetrahedron **1998**, *54*, 12985.
[7] E. Authority, EFSA Journal **2015**, *13*, 3991.
[8] M.V. Angelusiu, S.-F. Barbuceanu, C. Draghici, G.L. Almajan, Eur. J. Med. Chem. **2010**, *45*, 2055.
[9] H.G. Aslan, S. Özcan, N. Karacan, Inorg. Chem. Commun. **2011**, *14*, 1550.
[10] Z.-h. Xu, X.-w. Zhang, W.-q. Zhang, Y.-h. Gao, Z.-z. Zeng, Inorg. Chem. Commun. **2011**, *14*, 1569.
[11] M. Khalifa, Analusis**1995**, *23*, 453.
[12] O.A. El-Gammal, F.E. El-Morsy, B. Jeragh, A.A. El-Asmy, Can. Chem.Transac. **2013**, *1*, 277.
[13] M.A. Kabil, M.A. Akl, M.E. Khalifa, Anal. Sci. **1999**, *15*, 433.
[14] M. Katyal, Y. Dutt, Talanta**1975**, *22*, 151.
[15] A. Cameron, N. Gibson, R. Roper, Anal. Chim. Acta **1963**, *29*, 73.
[16] C. Bell, D. Rose, Talanta**1965**, *12*, 696.
[17] J. Sears, J. Darby, Mechanism of plasticizer action, in: N. Platzer (Ed.) The Technology of Plasticizers, **1982**, pp. 35.
[18] E. Massarani, D. Nardi, A. Tajana, L. Degen, J. Med. Chem. **1971**, *14*, 633.
[19] L. Troian-Gautier, C. Moucheron, Molecules **2014**, *19*, 5028.
[20] G.R. Reddy, S. Balasubramanian, RSC Advances **2015**, *5*, 53979.
[21] D. Ayodhya, M. Venkatesham, A.S. Kumari, G.B. Reddy, D. Ramakrishna, G. Veerabhadram, Journal of fluorescence **2015**, *25*, 1481.
[22] A. Guha, J. Adhikary, T.K. Mondal, D. Das, **2011**.
[23] **Modeling and Simulation Solutions for Chemicals and Materials Research**: BIOVIA Materials Studio, Accelrys software Inc., San Diego, USA, 2017.
[24] A.I. Vogel, Vogel'sTextbook of Quantitative Chemical Analysis, 5th ed., **1991**.
[25] X. Wu, A.K. Ray, Phys. Rev. B **2002**, *65*, 085403.
[26] B. Delley, D. Ellis, A. Freeman, E. Baerends, D. Post, Phys. Rev. B **1983**, *27*, 2132.
[27] B. Hammer, L.B. Hansen, J.K. Nørskov, Phys. Rev. B **1999**, *59*, 7413.
[28] A. Matveev, M. Staufer, M. Mayer, N. Rösch, Int. J. Quantum Chem **1999**, *75*, 863.
[29] A.K. Sadana, Y. Mirza, K.R. Aneja, O. Prakash, Eur. J. Med. Chem. **2003**, *38*, 533.
[30] S.M. Bridges, M.L. Salin, Plant Physiol. **1981**, *68*, 275.
[31] N.S. Burres, A. Frigo, R.R. Rasmussen, J.B. McAlpine, J. Nat. Prod. **1992**, *55*, 1582.
[32] T.A. Yousef, G.M. Abu El-Reash, R.M. El Morshedy, Polyhedron **2012**, *45*, 71.
[33] T.A. Yousef, G.M. Abu El-Reash, R.M. El Morshedy, J. Mol. Struct. **2013**, *1045*, 145.
[34] T. Yousef, G.A. El-Reash, O. El-Gammal, R. Bedier, J. Mol. Struct., 1029 (2012) 149-160.
[35] J.R. Ferraro, Low-frequency vibrations of inorganic and coordination compounds, Plenym press, New York, 1971.
[36] A.A.R. Despaigne, J.G. Da Silva, A.C.M. Do Carmo, O.E. Piro, E.E. Castellano, H. Beraldo, J. Mol. Struct. **2009**, *920*, 97.
[37] O. El-Gammal, G.A. El-Reash, M. El-Gamil, Spectrochim. Acta, A **2012**, *96*, 444.
[38] T.S. Lobana, P. Kumari, G. Hundal, R.J. Butcher, A. Castineiras, T. Akitsu, Inorg. Chim. Acta **2013**, *394*, 605.
[39] O.A. El-Gammal, G.M.A. El-Reash, M.M. El-Gamil, Spectrochimica Acta Part A: Molecular and Biomolecular Spectroscopy, 123 (2014) 59-70.
[40] T.S. Lobana, A. Sánchez, J.S. Casas, A. Castiñeiras, J. Sordo, M.S. García-Tasende, E.M. Vázquez-López, J. Chem. Soc., Dalton Trans. **1997**, 4289.
[41] C.M. Atta-ur-Rahman, W.J. Thomsen, Bioassay techniques for drug development, Harwood Academic Publishers, The Netherlands, **2001**.
[42] D.P. Riley, Chem. Rev. **1999**, *99*, 2573.